Limitations of 2-D Field Structure Assumptions in Electrical Properties Tomography and its 3-D CSI-EPT Solution

Fuchs, Patrick; Leijsen, Reijer; Remis, Rob

Publication date
2019

Document Version
Final published version

Published in
2nd International Workshop on MR-based Electrical Properties Tomography

Citation (APA)
Fuchs, P., Leijsen, R., & Remis, R. (2019). Limitations of 2-D Field Structure Assumptions in Electrical Properties Tomography and its 3-D CSI-EPT Solution. In *2nd International Workshop on MR-based Electrical Properties Tomography: March 13th-16th 2019 University Medical Center Utrecht The Netherlands*

Limitations of 2-D Field Structure Assumptions in Electrical Properties Tomography and its 3-D CSI-EPT Solution

P.S. Fuchs[1], R.L. Leijsen[2], and R.F. Remis[1]

[1]Circuits and Systems, Delft University of Technology, Delft, The Netherlands; [2]C.J.Gorter Center For High Field MRI, Leiden University Medical Center, Leiden, The Netherlands

Introduction

CSI-EPT is an Electrical Properties Tomography (EPT) reconstruction method that uses a Contrast Source Inversion (CSI) optimization approach to retrieve the conductivity and permittivity profiles of tissue based on B_1^+-data. The method can handle variations in tissue profiles and was originally implemented for profile reconstructions in the midplane of a birdcage coil, where the RF field exhibits an E-polarized field structure [1]. Recently, CSI-EPT has been extended to a fully 3-D volumetric reconstruction method that is generally applicable (in- or outside the midplane) and no particular field structure or smoothness is assumed [2]. This is a major step towards turning CSI-EPT into a practical reconstruction method. Unfortunately, the computation times significantly increase (hours or even days, depending on the reconstruction domain of interest) and from this point of view a 2-D approach may be preferable. We show, however, that a 2-D approach is only warranted under very specific circumstances and having an E-polarized field structure is a necessary but not sufficient condition. In particular, we show that to obtain accurate tissue reconstructions based on 3-D B_1^+-data, it is in general necessary to take all electromagnetic field components into account and a 2-D reconstruction approach will lead to reconstruction artefacts.

Methods

We use 2-D and 3-D CSI-EPT to reconstruct tissue profiles within a realistic male head model (Virtual Family [4]) consisting of 124x100x109 voxels (2x2x2 mm [3]; Model A, Figure 1a). To investigate the consequences of a 2-D assumption, a longitudinal homogeneous head model (Model B, Figure 1b) is considered as well in which the center slice is extended in the longitudinal direction. The RF fields are generated by an ideal birdcage coil driven in quadrature at 128 MHz and are computed using XFdtd software (Remcom [5]).

In CSI-EPT an objective function is minimized, which consists of a data and consistency mismatch term. The modeled data is computed as

$$B_1^{+;\mathrm{sc}} = \frac{\omega}{c_0^2}(\partial^+ A_z^{\mathrm{sc}} - \partial_z A^{+;\mathrm{sc}}) \quad \text{[3-D]} \quad \text{and} \quad B_1^{+;\mathrm{sc}} = \frac{\omega}{c_0^2}\partial^+ A_z^{\mathrm{sc}}, \quad \text{[2-D]}$$

which are obtained from the Maxwell field representations

$$\boldsymbol{B}^{\mathrm{sc}} = \mathrm{j}\frac{\omega}{c_0^2}\nabla \times \boldsymbol{A}^{\mathrm{sc}} \quad \text{[3-D]} \quad \text{and} \quad \boldsymbol{B}^{\mathrm{sc}} = \mathrm{j}\frac{\omega}{c_0^2}\nabla_T \times \boldsymbol{A}^{\mathrm{sc}}. \quad \text{[2-D]}$$

The consistency term is evaluated using

$$\boldsymbol{E}^{\mathrm{sc}} = (k_0^2 + \nabla\nabla\cdot)\boldsymbol{A}^{\mathrm{sc}} \quad \text{[3-D]} \quad \text{and} \quad \boldsymbol{E}^{\mathrm{sc}} = \mathrm{k}_0^2\boldsymbol{A}^{\mathrm{sc}}. \quad \text{[2-D]}$$

Here, $\boldsymbol{A}^{\mathrm{sc}}$ is the scattered electric vector potential, $A^{+;\mathrm{sc}} = \frac{1}{2}(A_x^{\mathrm{sc}} + jA_y^{\mathrm{sc}})$, ∇_T the transverse nabla operator, and k_0 the wave number of the surrounding medium. From these representations it is immediately clear that the gradient-divergence term in the E-field representation is absent in 2-D as opposed to a 3-D formulation and longitudinal variations of the vector potential are also ignored.

Results and Discussion

In model B, the 3-D field indeed has an E-polarized field structure in the center slice (top row, Figure 2a--c). For model A, the electric field has non-negligible transverse components in this slice (bottom row, Figure 2a--c), which are absent for a purely E-polarized field. In a slice five centimeters above the center slice, however, E-polarized field structure is completely lost for both head models (Figure 2d--f) showing that there are longitudinal variations. Figure 3 confirms these findings by showing the magnitude of the x- and y-components of the E-field relative to the magnitude of its -component. Only in the center slice for a z-invariant object the x- and y-components of the electric field may be neglected.

Furthermore, in Figure 4a we show the B_1^+ field distribution in the center slice for a 2-D setup, where both the model and the rungs of the coil extend to infinity in the longitudinal direction and compare this 2-D field with the B_1^+-field obtained with Model B and long but finite rung lengths in the longitudinal direction (Figure 4b). In this case, the B_1^+-field structure is similar to a 2-D field structure. However, if we replace the “long-rung coil” by a realistic coil, but keep Model B, the B_1^+-field pattern starts to

change (Figure 4c). For Model A, large deviations in the B_1^+-field pattern are observed compared with its 2-D counterpart (Figure 4d).
Finally, Figure 5 shows the 2-D and 3-D conductivity and permittivity reconstructions for both models within the center slice and a slice 5 centimeters above. We observe that if 2-D CSI-EPT is used, large reconstruction errors are obtained and only 3-D CSI-EPT is able to accurately reconstruct the tissue profiles.

Conclusion

Reliable tissue reconstructions can be obtained with 3-D CSI-EPT without making invariance or smoothness assumptions. Its 2-D counterpart is computationally more efficient, but we have shown that its applicability is rather limited and similarities between 2-D and 3-D field structures are not sufficient for 2-D CSI-EPT. The computational costs of 3-D CSI-EPT can be alleviated by including preconditioning techniques and improved initial guesses. Future work will focus on turning 3-D CSI-EPT into a clinically applicable EPT imaging modality by incorporating these techniques along with coil loading effects and transceive phase correction mechanisms.

References

[1] Balidemaj, IEEE Tran Med Im, 2015; [2] Leijsen, IEEE Tran Med Im, 2018; [3] Fuchs, IEEE Tran Comp Im, 2018; [4] Christ, Phys Med Biol, 2010; [5] XFdtd, Remcom State College, PA, USA.

Acknowledgements

The research of P.S. Fuchs was funded in part through a collaboration between the Delft University of Technology and the Indian Institute of Science. The research of R.L. Leijsen was funded by European Research Council Advanced NOMA MRI under grant number 670629.

Figures

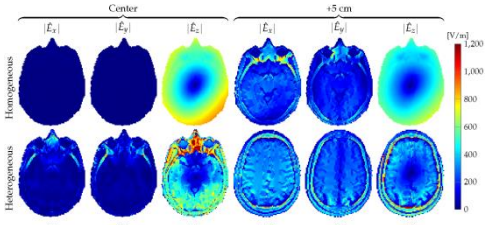

Figure 2: Magnitude of the electric field strength component at two positions in the birdcage coil (for the midplane, (a-c) and five centimeters above the midplane (d-f)) and for a longitudinal homogeneous head (model B, top row) and heterogeneous head (model A, bottom row).

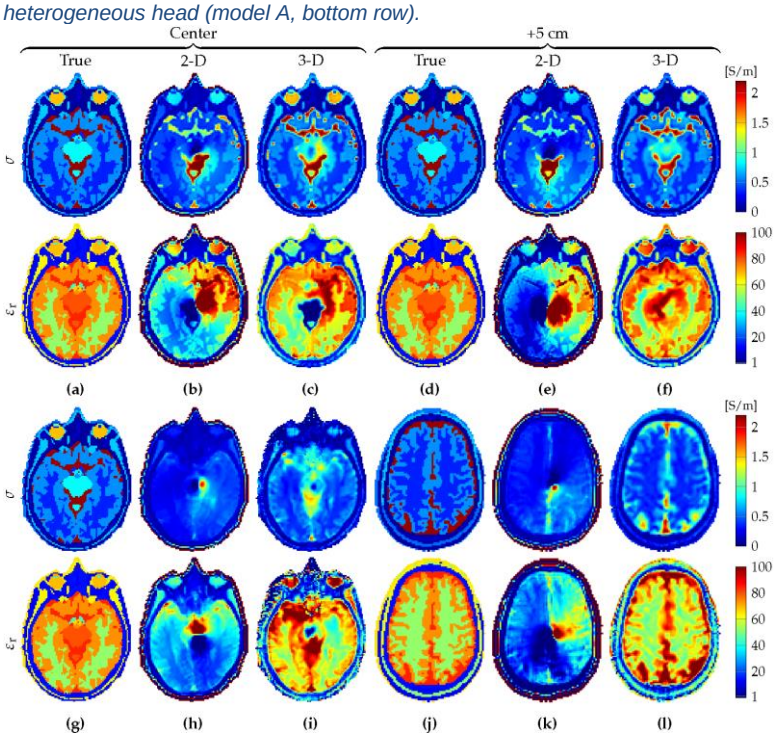

Figure 5: Reconstructions with 2-D and 3-D CSI-EPT for fully 3-D simulated fields, for both model A (g-l) and model B (a-f) at two different locations in a birdcage coil.

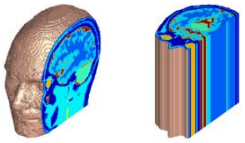

Figure 1: The two head models. (a) is the Duke model from the Virtual Family[4] (model A) and (b) is the longitudinally "stretched" center slice variant to ensure z-translation invariance (model B).

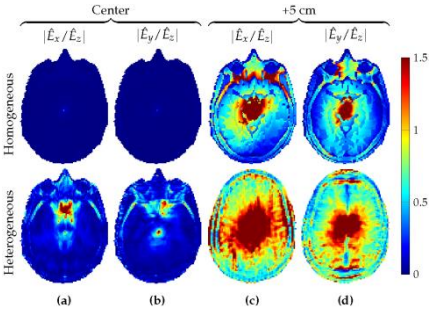

Figure 3: The x- and y-components of the electric field strength relative to its z-component at the midplane and five centimeters above the midplane of the birdcage coil and for two different models.

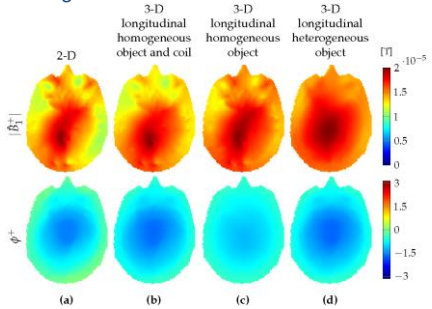

Figure 4: B_1^+-field distributions for 2-D (a), quasi-3-D (b,c) and 3-D settings (d). The assumed B_1^+-fields of a 2-D approach in the center of a BC coil are clearly different from a 3-D setting.